ELSEVIER

International Journal of Heat and Fluid Flow 20 (1999) 60–67

International Journal of HEAT AND FLUID FLOW

# Heat transfer to viscoplastic materials flowing laminarly in the entrance region of tubes

Márcia Soares, Mônica F. Naccache, Paulo R. Souza Mendes *

*Department of Mechanical Engineering, Pontifícia Universidade Católica, Rio de Janeiro, RJ 22453-900, Brazil*

Received 29 October 1997; accepted 2 September 1998

**Abstract**

Heat transfer in the entrance-region flow of viscoplastic materials inside tubes is analyzed. The flow is laminar and the material viscosity is modeled by the Herschel–Bulkley equation. The conservation equations are solved numerically via a finite volume method. Two different thermal boundary conditions are considered, namely, uniform wall temperature and uniform wall heat flux. The effect of temperature-dependent properties is also investigated. The Nusselt number is obtained as a function of the axial coordinate, yield stress, and power-law exponent. Results show that the same trend is observed for the two thermal boundary conditions, but the Nusselt numbers are always higher for the isoflux-wall cases. The length of the entrance region decreases as the material behavior departs from the Newtonian one. Finally, it is observed that neglecting the temperature dependence of material properties may introduce important errors in the heat transfer coefficient. 

*Keywords:* Flow of viscoplastic materials; Forced convection through short ducts; Herschel–Bulkley materials

## Notation

| | |
|---|---|
| $a$ | sensitivity of yield stress to temperature, $\equiv -(\mathrm{d}\tau_0/\mathrm{d}T)/\tau_0$ (1/K) |
| $b$ | sensitivity of consistency index to temperature, $\equiv -(\mathrm{d}K/\mathrm{d}T)/K$ (1/K) |
| $c$ | specific heat (J/kg K) |
| $D$ | tube diameter (m) |
| $f$ | friction factor, $\equiv (2(\partial p/\partial x)D)/(\rho\bar{u}^2)$ |
| $h$ | heat transfer coefficient (W/m$^2$ K) |
| $K$ | consistency index (kg/m s$^{2-n}$) |
| $K_{\mathrm{ref}}$ | consistency index at reference temperature (kg/m s$^{2-n}$) |
| $n$ | power-law exponent |
| Nu | Nusselt number, $\equiv hD/\kappa$ |
| $p$ | pressure (Pa) |
| $p'$ | dimensionless pressure |
| Pe | Peclet number, $\equiv \bar{u}D/\alpha$ |
| Pr | Prandtl number, $\eta_c c/\kappa$ |
| $q_w$ | wall heat flux (W/m$^2$) |
| $r$ | radial coordinate (m) |
| $r'$ | dimensionless radial coordinate, $\equiv r/R$ |
| $R$ | tube radius (m) |
| Re | Reynolds number, $\equiv \rho\bar{u}D/\eta_c$ |
| $T$ | temperature field (°C) |
| $T_b$ | bulk temperature (°C) |
| $T_i$ | inlet temperature (°C) |
| $T_{\mathrm{ref}}$ | reference temperature (°C) |
| $T_w$ | wall temperature (°C) |
| $u$ | $x$-component of velocity (m/s) |
| $\bar{u}$ | mean axial velocity (m/s) |
| $u'$ | dimensionless $x$-component of velocity, $\equiv u/\dot{\gamma}_c R$ |
| $\bar{u}'$ | dimensionless mean axial velocity, $\equiv \bar{u}/\dot{\gamma}_c R$ |
| $\mathbf{v}$ | velocity vector (m/s) |
| $v$ | $r$-component of velocity (m/s) |
| $v'$ | dimensionless $r$-component of velocity, $\equiv v/\dot{\gamma}_c R$ |
| $x$ | axial coordinate (m) |
| $x'$ | dimensionless axial coordinate, $\equiv x/R$ |
| $x^+$ | inverse Graetz number, $\equiv x'/\mathrm{Pe}$ |

*Greek*

| | |
|---|---|
| $\alpha$ | thermal diffusivity, $\equiv \kappa/\rho c$ (m$^2$/s) |
| $\dot{\gamma}$ | deformation rate, $\equiv \sqrt{\frac{1}{2}\mathrm{tr}\dot{\boldsymbol{\gamma}}^2}$ (s$^{-1}$) |
| $\dot{\gamma}'$ | dimensionless deformation rate, $\equiv \dot{\gamma}/\dot{\gamma}_c$ |
| $\dot{\gamma}_c$ | characteristic deformation rate (s$^{-1}$) |
| $\dot{\boldsymbol{\gamma}}$ | rate-of-deformation tensor (s$^{-1}$) |
| $\eta$ | viscosity function (kg/m s) |
| $\eta'$ | dimensionless viscosity function, $\equiv \eta/\eta_c$ |
| $\eta_c$ | characteristic viscosity (kg/m s) |
| $\kappa$ | thermal conductivity (W/m K) |
| $\theta$ | dimensionless temperature, $\equiv (T - T_w)/(T_i - T_w)$ |
| $\rho$ | mass density (kg/m$^3$) |
| $\tau$ | magnitude of the extra-stress tensor, $\equiv \sqrt{\frac{1}{2}\mathrm{tr}\boldsymbol{\tau}^2}$ (Pa) |
| $\tau_0$ | yield stress (Pa) |
| $\tau_{0\mathrm{ref}}$ | yield stress at reference temperature (Pa) |
| $\boldsymbol{\tau}$ | extra-stress tensor (Pa) |
| $\Phi$ | dimensionless temperature, $\equiv (T - T_i)/(q_w D/\kappa)$ |

* Corresponding author. E-mail: pmendes@mec.puc-rio.br.

0142-727X/99/$ – see front matter 
PII: S0142-727X(98)10044-9

## 1. Introduction

There are a large number of industrial processes, such as the ones found in the industries of petroleum, cosmetics, foods, plastics, paints and pharmaceutical, that somehow deal with viscoplastic materials. Frequently, these processes involve non-isothermal situations, and the temperature distribution in the material must be known in order to allow control of its rheology.

An important example is found in the process of drilling petroleum wells. Drill muds have a key role in this process. They are typically concentrated suspensions, and, consequently, highly non-Newtonian in nature. They should have the correct density to provide the pressure needed for well integrity and for avoiding premature production of hydrocarbons. Their rheological properties must be such as to allow carrying rock particles that are generated during drill operation, with a minimum of pumping power. This requires a highly shear-thinning rheological behavior. Also, the success of a well cementing operation depends to a great extent on the knowledge and control of the cement rheological properties. Because the material properties are strong functions of temperature, and because these flows are not isothermal, heat transfer information is needed to allow reliable designs of such costly drilling or cementing operations.

Heat transfer to Bingham plastics and power-law fluids in laminar flow through tubes has been investigated to some extent. Bird et al. (1983) presented an overview of the rheology and flow of viscoplastic materials, and analyzed some simple flow situations using a Generalized Newtonian Liquid (GNL) model with a Bingham plastic viscosity function. For fully developed laminar flow of power-law fluids in tubes, Bird et al. (1987) gave Nu = 3.657, 3.949 and 4.175, respectively, for the power-law exponent $n = 1$, 0.5 and 1/3 and uniform wall temperature. For uniform wall heat flux, an analytical solution is easily obtained (Irvine and Karni, 1987)

$$\mathrm{Nu} = \frac{8(5n+1)(3n+1)}{31n^2+12n+1}. \quad (1)$$

A comprehensive research focusing on the heat transfer problem in the developing flow of power-law fluids through tubes has been performed by Joshi and Bergles (1980a, b). In this study, they obtained correlations for $q_w$ =constant, and considered the temperature dependence of $K$. Another experimental study for flow and heat transfer to pseudoplastic materials is presented by Scirocco et al. (1985). In both studies, at the inlet of the heated portion of the test section the velocity profiles are already fully developed. Richardson (1987) presents asymptotic solutions for power-law fluids considering a temperature-dependent consistency index. Vradis et al. (1992) analyzed the heat transfer problem in the simultaneously developing flow of a Bingham material, assuming uniform wall temperature and constant thermophysical properties. In this numerical study, axial conduction is neglected. The analysis reported by Blackwell (1985) for Bingham materials also assumes constant properties and uniform wall temperature. Moreover, axial conduction is also neglected, and the flow is considered hydrodynamically developed from the tube inlet.

Forrest and Wilkinson (1973), and, more recently, Nouar et al. (1994), studied the heat transfer problem of the Herschel–Bulkley materials flowing inside tubes. These works considered hydrodynamic development from the tube inlet, and neglected axial conduction. In Forrest and Wilkinson's numerical study, both the uniform wall heat flux and the uniform wall temperature thermal boundary conditions have been investigated. Nouar et al. (1994) reported a theoretical and experimental study, considering a constant wall heat flux boundary condition. In this paper, the impact on velocity profiles and Nusselt numbers of temperature-dependent rheological properties is discussed. In a similar study, Nouar et al. (1995) obtained numerical results assuming fully developed flow at the entrance of the heated region. Axial conduction was neglected, and the temperature dependence of the consistency index was considered. Correlations for friction factor and Nusselt number were also proposed.

For turbulent flow, the thermal boundary condition assumes minor importance, and the entry length becomes much shorter. Moreover, the shear rates are so large that the yield stress limit becomes unimportant. Therefore, information for power-law fluids and for fully developed flow can be employed for a wide range of situations. Irvine and Karni (1987) recommend Yoo's correlation, valid in the range $0.2 \leqslant n \leqslant 0.9$:

$$j_H \equiv \frac{\mathrm{Nu}}{\mathrm{Re}\,\mathrm{Pr}^{1/3}} = \frac{0.0152}{\mathrm{Re}^{0.155}}, \quad (2)$$

where

$$\mathrm{Re} = \frac{\rho \bar{u}^{2-n} D^n}{K}\left(\frac{2(3n+1)}{n}\right)^{1-n} \quad (3)$$

and

$$\mathrm{Pr} = \frac{Kc}{\kappa}\left(\frac{(3n+1)}{4n}\right)^{n-1}\left(\frac{8\bar{u}}{D}\right)^{n-1}. \quad (4)$$

In the above expressions, $D$ is the tube diameter, $\rho$ the mass density, $\bar{u}$, the average velocity, $c$, the specific heat, and $\kappa$ the thermal conductivity. Yoo's correlation can be used for Re's in the range $3000 \leqslant \mathrm{Re} \leqslant 90000$. From Eq. (2), it can be seen that $j_H$ is a rather weak function of Re.

Another important point discussed in the literature of viscoplastic materials is the numerical difficulty in using the von Mises yield criterion. Essentially two types of modification of the Bingham plastic viscosity function have been proposed to handle this, namely, the bi-viscosity model (Lipscomb and Denn, 1984; Gartling and Phan-Thien, 1984; O'Donovan and Tanner, 1984), and Papanastasiou's model (Papanastasiou, 1987). Both modifications have been used successfully in analyses and numerical simulations of different complex flows (e.g., Ellwood et al., 1990; Abdali et al., 1992; Beverly and Tanner, 1992; Wilson, 1993; Wilson and Taylor, 1996; Piau, 1996).

In the present work, laminar heat transfer coefficients for entrance-region flows through tubes of viscoplastic materials are presented. Numerical results for both the isothermal-wall ($T_w$ = constant) and the isoflux-wall ($q_w$ = constant) thermal boundary conditions are obtained. The case of simultaneous velocity and temperature development is considered, and axial conduction is accounted for in the analysis. The mechanical behavior of the material is assumed to be well represented by the Generalized Newtonian Liquid model (GNL), which gives excellent results when the main goal is to obtain a flow rate/pressure drop, or flow rate/drag force relationship. In this model, the extra-stress tensor $\boldsymbol{\tau}$ is given by

$$\boldsymbol{\tau} = \eta \dot{\boldsymbol{\gamma}}. \quad (5)$$

In the above equation, $\dot{\boldsymbol{\gamma}}$ is the rate-of-deformation tensor, defined as grad $\mathbf{v}$ + (grad $\mathbf{v}$)$^T$, where $\mathbf{v}$ is the velocity vector. The quantity $\eta$ is the viscosity function, assumed here to be of the Herschel–Bulkley form

$$\eta = \begin{cases} \tau_0/\dot{\gamma} + K\dot{\gamma}^{n-1} & \text{if } \tau > \tau_0, \\ \infty & \text{otherwise.} \end{cases} \quad (6)$$

In Eq. (6), $\tau_0$ is the yield stress, $\tau \equiv \sqrt{\frac{1}{2}\mathrm{tr}\boldsymbol{\tau}^2}$ a measure of the magnitude of $\boldsymbol{\tau}$, $\dot{\gamma} \equiv \sqrt{\frac{1}{2}\mathrm{tr}\,\dot{\boldsymbol{\gamma}}^2}$ a measure of the magnitude of $\dot{\boldsymbol{\gamma}}$, $K$ the consistency index, and $n$the power-law exponent. Typically $K$ and $\tau_0$ are sensitive to the temperature of the material. However, for drilling muds and cements, the power-law exponent, $n$, is often independent of temperature variations. These three parameters ($\tau_0$, $K$ and $n$) are normally determined via least squares fits to experimental shear ($\tau \times \dot{\gamma}$) data. In most of the present work, these rheological parameters were assumed to be independent of temperature. However, in order to assess the validity of this assumption, some results were obtained assuming that $\tau_0$ and $K$ are the following functions of temperature:

$$\tau_0 = \tau_{0\mathrm{ref}} \mathrm{e}^{-a(T-T_{\mathrm{ref}})}, \tag{7}$$

$$K = K_{\mathrm{ref}} \mathrm{e}^{-b(T-T_{\mathrm{ref}})}. \tag{8}$$

In these equations, $\tau_{0\mathrm{ref}}$ and $K_{\mathrm{ref}}$ are the values of $\tau_0$ and $K$ at a reference temperature, which was chosen to be the inlet temperature for the cases with uniform wall heat flux, and the wall temperature for the uniform wall temperature cases. The reference values and parameters $a$ and $b$ were obtained via least-squares fits to measured data for mayonnaise (Soares, 1996).

Results are presented in terms of velocity, pressure and temperature fields. The variation of the heat transfer coefficient with the inverse Graetz number and some rheological parameters are also presented. As far as the authors know, this is the first heat transfer study of laminar entry-region flow of viscoplastic materials through tubes which considers the simultaneous hydrodynamic and thermal development.

## 2. Analysis

In the analysis, the flow is assumed to be steady and axisym metric. The hypothesis of constant thermophysical properties is also employed. The mass, momentum and energy conservation equations, in conjunction with the GNL (Eq. (5)) constitutive equation and appropriate boundary conditions, govern this physical situation.

In order to obtain representative dimensionless governing equations and dimensionless parameters, the choice of characteristic quantities is crucial. For this problem, it is appropriate to choose fully developed values of some key quantities as characteristic quantities, as discussed next.

The characteristic shear rate, $\dot{\gamma}_c$, is chosen to be the one that occurs at the tube wall in the fully developed region, and at the reference temperature:

$$\dot{\gamma}_c \equiv \left( \frac{\tau_{R,\mathrm{fd}} - \tau_{0\mathrm{ref}}}{K_{\mathrm{ref}}} \right)^{1/n}, \tag{9}$$

where $\tau_{R,\mathrm{fd}}$ is the shear stress at the wall in the fully developed region, which can be easily related to the pressure drop by means of a force balance:

$$\tau_{R,\mathrm{fd}} \equiv -[\tau_{rx}(R)]_{\mathrm{fd}} = -\left( \frac{\mathrm{d}p}{\mathrm{d}x} \right)_{\mathrm{fd}} \frac{R}{2} = \frac{\Delta p}{L_{\mathrm{fd}}} \frac{R}{2}. \tag{10}$$

The subscript "fd" indicates that the quantity is to be evaluated in the fully developed region. In the above expression, $p$ is the pressure, $x$ the axial coordinate, $R$ the tube radius, and $L_{\mathrm{fd}}$ a tube length in the fully developed region to whose ends the pressure difference $\Delta p$ corresponds.

The characteristic viscosity is chosen as

$$\eta_c \equiv \eta(\dot{\gamma}_c) = \frac{\tau_{R,\mathrm{fd}}}{\dot{\gamma}_c}. \tag{11}$$

The dimensionless shear rate and viscosity are respectively defined as

$$\dot{\gamma}' \equiv \dot{\gamma}/\dot{\gamma}_c, \qquad \eta' \equiv \eta/\eta_c. \tag{12}$$

Using the above definitions, the dimensionless viscosity function can be written as

$$\eta' = \begin{cases} r'_0/\dot{\gamma}' + (1-r'_0)\dot{\gamma}'^{\,n-1} & \text{if } \tau' > r'_0, \\ \infty & \text{otherwise.} \end{cases} \tag{13}$$

where

$$\tau' \equiv \frac{\tau}{\tau_{R,\mathrm{fd}}} \text{ and } r'_0 \equiv \frac{r_0}{R} = \frac{\tau_{0\mathrm{ref}}}{\tau_{R,\mathrm{fd}}}. \tag{14}$$

A result of interest is the expression for the fully developed wall shear rate, $\dot{\gamma}_c$:

$$\dot{\gamma}_c = \frac{\bar{u}}{\bar{u}'R} = \frac{\bar{u}}{R} \frac{n+1}{2n} \left[ \frac{1}{2}(1-r'_0) - \frac{n}{2n+1}(r'_0)(1-r'_0)^2 - \frac{n}{3n+1}(1-r'_0)^3 \right]^{-1}. \tag{15}$$

In this equation $\bar{u}$ is the average velocity and $\bar{u}'$ the corresponding dimensionless quantity, given by $\bar{u}' \equiv \bar{u}/R\dot{\gamma}_c$ (Souza et al., 1995; Soares et al., 1997). Clearly, the above equation can be rewritten as a useful relationship between flow rate and pressure drop. It is also interesting to observe that it reduces to the well-known expressions for the wall shear rate for fully developed flow of power-law ($r'_0 = 0$) and Newtonian ($r'_0 = 0, n = 1$) fluids, namely

$$\dot{\gamma}_{c,\ \text{power-law}} = \left( \frac{8\bar{u}}{D} \right) \frac{3n+1}{4n},$$
$$\dot{\gamma}_{c,\ \text{Newtonian}} = \left( \frac{8\bar{u}}{D} \right). \tag{16}$$

### 2.1. Conservation of mass and momentum

Using the above defined characteristic quantities, the conservation equations can be reduced to their dimensionless forms. The mass and momentum equations for the entrance region of a steady laminar flow of a Herschel–Bulkley material through a duct are thus given by

$$\frac{\partial u'}{\partial x'} + \frac{1}{r'} \frac{\partial (r'v')}{\partial r'} = 0, \tag{17}$$

$$v' \frac{\partial u'}{\partial r'} + u' \frac{\partial u'}{\partial x'} = -\frac{\partial p'}{\partial x'} + \frac{2\bar{u}'}{\mathrm{Re}} \left[ \frac{1}{r'} \frac{\partial}{\partial r'} \left( \eta' r' \frac{\partial u'}{\partial r'} \right) + \frac{\partial}{\partial x'} \left( \eta' \frac{\partial u'}{\partial x'} \right) \right], \tag{18}$$

$$v' \frac{\partial v'}{\partial r'} + u' \frac{\partial v'}{\partial x'} = -\frac{\partial p'}{\partial r'} + \frac{2\bar{u}'}{\mathrm{Re}} \left[ \frac{\partial}{\partial r'} \left( \frac{1}{r'} \frac{\partial}{\partial r'} (\eta' r' v') \right) + \frac{\partial}{\partial x'} \left( \eta' \frac{\partial v'}{\partial x'} \right) \right]. \tag{19}$$

In these equations, $v' = v/R\dot{\gamma}_c$, $x' = x/R$, $r' = r/R$, and $p' = p/\rho(R\dot{\gamma}_c)^2$. The Reynolds number is defined as

$$\mathrm{Re} \equiv \frac{\rho \bar{u} D}{\eta_c} = \frac{2\rho(\bar{u}')^{n-1}(\bar{u})^{2-n} R^n}{K_{\mathrm{ref}} + \tau_{0\mathrm{ref}}(\bar{u}')^n R^n/(\bar{u})^n}. \tag{20}$$

It is interesting to observe that, when $\tau_{0\mathrm{ref}} = 0$, Eq. (20) reduces to Eq. (3), which is a widely used expression for the Reynolds number for flows of power-law fluids, and which is often incorrectly used for flows of viscoplastic materials as well.

The boundary conditions are the usual no-slip condition at the wall, the symmetry condition at the centerline, uniform velocity profile at the tube inlet, and locally parabolic flow at the outlet:

$$\begin{aligned} &\frac{\partial u'}{\partial r'}(0,x')=0, \quad v'(0,x')=0,\\ &u'(1,x')=0, \quad v'(1,x')=0,\\ &u'(r',0)=\bar{u}', \quad v'(r',0)=0,\\ &\frac{\partial u'}{\partial x'}(r',L')=0, \quad \frac{\partial v'}{\partial x'}(r',L')=0; \end{aligned} \tag{21}$$

where $L' \equiv L/R$ is the dimensionless tube length.

### 2.2. Modified bi-viscosity model

The viscosity function as given by Eq. (13) is not convenient to handle numerically. The usual approach in numerical schemes for flows of Bingham plastics is to replace it with another viscosity function, the so-called *bi-viscosity model* (Beverly and Tanner, 1992). This idea can be easily extended to Herschel–Bulkley materials, yielding the following approximate representation of the viscosity function:

$$\eta' = \begin{cases} r'_0/\dot{\gamma}' + (1-r'_0)\dot{\gamma}'^{n-1} & \text{if } \dot{\gamma}' > \dot{\gamma}'_{\text{small}},\\ \eta'_{\text{large}} & \text{otherwise.} \end{cases} \tag{22}$$

For the case of Bingham materials Beverly and Tanner (1992) recommend

$$\eta'_{\text{large}} = 1000. \tag{23}$$

This value is also employed here. Therefore,

$$\dot{\gamma}'_{\text{small}} = \frac{r'_0}{1000-(1-r'_0)\dot{\gamma}'^{n-1}_{\text{small}}} \simeq \frac{r'_0}{1000}. \tag{24}$$

### 2.3. Conservation of energy

Neglecting viscous dissipation effects and assuming that the thermal conductivity is constant, the dimensionless energy equation for the thermal boundary condition of uniform wall temperature is given by

$$u'\frac{\partial\theta}{\partial x'} + v'\frac{\partial\theta}{\partial r'} = \frac{2\bar{u}'}{\text{Pe}}\left\{\frac{\partial^2\theta}{\partial x'^2} + \frac{1}{r'}\frac{\partial}{\partial r'}\left(r'\frac{\partial\theta}{\partial r'}\right)\right\}, \tag{25}$$

where $\theta \equiv (T-T_w)/(T_i-T_w)$, $\text{Pe} \equiv \bar{u}D/\alpha$ the Peclet number, and $\alpha \equiv \kappa/(\rho c)$ the thermal diffusivity.

Similarly, for the thermal boundary condition of uniform wall heat flux,

$$u'\frac{\partial\Phi}{\partial x'} + v'\frac{\partial\Phi}{\partial r'} = \frac{2\bar{u}'}{\text{Pe}}\left\{\frac{\partial^2\Phi}{\partial x'^2} + \frac{1}{r'}\frac{\partial}{\partial r'}\left(r'\frac{\partial\Phi}{\partial r'}\right)\right\}, \tag{26}$$

where $\Phi \equiv (T-T_i)/(q_w D/\kappa)$.

From Eqs. (25) and (26), it can be seen that, when viscous dissipation effects are negligible, the influence of rheological behavior on heat transfer is conveyed through the velocity field only.

For uniform wall temperature, the boundary conditions for Eq. (25) are

$$\begin{aligned} &\frac{\partial\theta}{\partial r'}(0,x')=0, \quad \theta(1,x')=0,\\ &\theta(r',0)=1, \quad \frac{\partial\theta}{\partial x'}(r',L')=0; \end{aligned} \tag{27}$$

while, for uniform wall heat flux, the thermal boundary conditions should be written as

$$\begin{aligned} &\frac{\partial\Phi}{\partial r'}(0,x')=0, \quad \frac{\partial\Phi}{\partial r'}(1,x')=1,\\ &\Phi(r',0)=0, \quad \frac{\partial\Phi}{\partial x'}(r',L')=\frac{2}{\text{Pe}}. \end{aligned} \tag{28}$$

It should be clear that the above boundary conditions at $L$ have no physical basis whatsoever, but are needed in numerical integrations where outflow boundaries are present. If used appropriately, however, they typically yield excellent results.

For the uniform wall temperature boundary condition, the Nusselt number is given by

$$\text{Nu}(x') \equiv \frac{hD}{\kappa} = -\frac{2}{\theta_b(x')}\frac{\partial\theta}{\partial r'}(1,x'), \tag{29}$$

where $\theta_b$ is the dimensionless bulk temperature, defined as

$$\theta_b \equiv 2\int_0^1 \frac{u'}{\bar{u}'}\theta r'\,dr'. \tag{30}$$

When the thermal boundary condition at the tube wall is one of the uniform heat flux, the Nusselt number becomes

$$\text{Nu}(x') \equiv \frac{hD}{\kappa} = -\frac{1}{(\Phi_w(x')-\Phi_b(x'))}, \tag{31}$$

where

$$\Phi_b \equiv 2\int_0^1 \frac{u'}{\bar{u}'}\Phi r'\,dr'. \tag{32}$$

### 2.4. Numerical solution

The conservation equations are discretized by the finite volume method described by Patankar (1980). Staggered velocity components are employed to avoid unrealistic pressure fields. The pressure–velocity coupling is handled by the SIMPLEC algorithm (Van Doormaal and Raithby, 1984). The resulting algebraic system is solved by the TDMA line-by-line algorithm (Patankar, 1980) with the block correction algorithm (Settari and Aziz, 1973) to increase the convergence rate.

A non-uniform $140 \times 32$ grid is employed, with points concentrated toward the inlet region in the $x$-direction, and toward the wall in the $r$-direction, to resolve the sharp gradients expected at these locations. The domain length in the axial direction, $L$, is equal to fifteen diameters for the low Pe cases, and ninety-five diameters for the high Pe cases.

Extensive grid tests were performed, which attested that the solutions obtained are grid-independent. Two kinds of tests, for the Newtonian and the Herschel–Bulkley materials, were done. The results obtained were compared with the values presented in the literature and with the results for finer meshes. For the flow of a Newtonian fluid ($\text{Pe}=50$ and $\text{Re}=10$), fully developed value of Nusselt number is less than 0.1% different from the exact value, presented in Shah and London (1978). The same error occurs for the fully developed value of the product between the friction factor and the Reynolds number, $f\,\text{Re}$. The average value of the errors for the fully developed local axial velocities with respect to the analytical solution is equal to 0.07% for the mesh used ($140 \times 32$). However, it is interesting to note that the length of the entrance region is rather sensitive to mesh refinement. Refining the grid to $175 \times 62$ decreases it by 8%.

For a Herschel–Bulkley material ($n=0.3$; $r'_0=0.3$), the differences between the $140 \times 32$ and the $175 \times 62$ grid are 0.3% for the $f\,\text{Re}$, 0.24% for the Nusselt number and 5.72% for the length of the entrance region. Comparing the results obtained for the fully developed velocity profiles with the analytical solution (Souza et al., 1995), the agreement is excellent, with an average error of 1.14%

A detailed comparison with results available in the literature for some particular cases for the purpose of validation can be found in Soares (1996). As an example, Nu results obtained for a power-law fluid are compared with the ones given by Joshi and Bergles (1980a) in Fig. 1. It can be seen in this figure

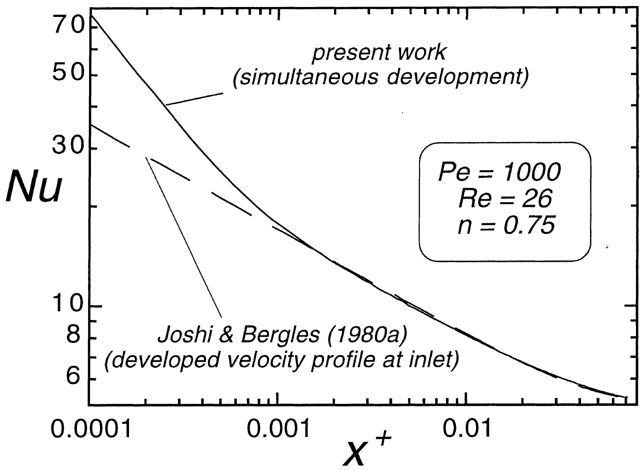


Fig. 1. Comparison of predictions with experimental results.

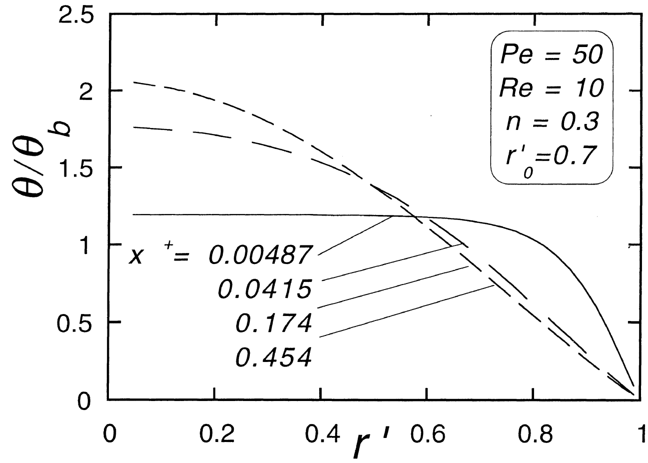


Fig. 3. Temperature profiles: Herschel–Bulkley material ($T_w$ = const.).

that the agreement is quite good, except in a short region starting at the entrance of the tube. The departure is due to the different hydrodynamic inlet condition imposed by Joshi and Bergles (1980a) – fully developed flow, as opposed to the uniform velocity profile.

### 3. Results and discussion

Because this problem is governed by an exceedingly large number of parameters, an extensive parametric analysis is not practical. Therefore, only a few representative combinations of the governing parameters are examined.

Fig. 2 shows velocity profiles at four different axial positions along the entrance region. It is seen that, close to the tube inlet, there is a velocity overshoot near the wall. This overshoot is related to axial diffusion of momentum, and therefore cannot be predicted by formulations that consider radial diffusion only. Although milder than the one observed for Newtonian fluids, this effect is not negligible, and might have an important impact in heat transfer.

The results shown in Figs. 3–7 pertain to the uniform wall temperature boundary condition. Temperature profiles at some axial locations are seen in Fig. 3. In order to eliminate the $x$-dependence in the fully developed region, these profiles are presented as a ratio of $\theta$ to $\theta_b$. Because the Prandtl number, defined as $\mathrm{Pr} \equiv \eta_c/\rho\alpha = \mathrm{Pe}/\mathrm{Re}$, is equal to 5, the thermal development lengths are larger than the corresponding hydrodynamic development lengths, indicated in Fig. 2.

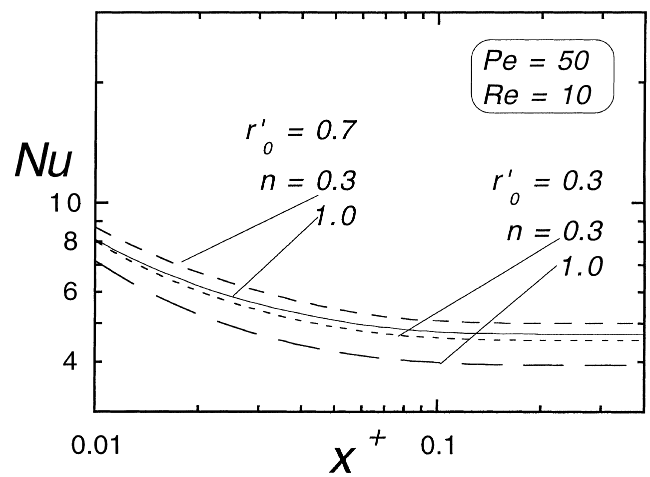


Fig. 4. Entrance-region Nu for different $r_0'$'s and $n$'s ($T_w$ = const.).

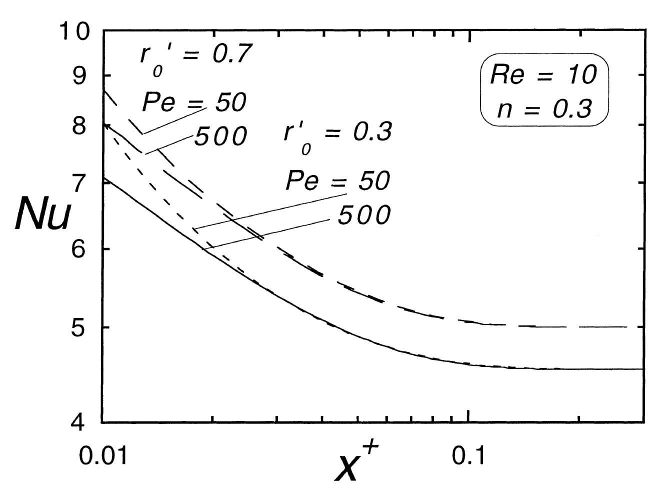


Fig. 5. Entrance-region Nu for different $r_0'$'s and Pe's ($T_w$ = const.).

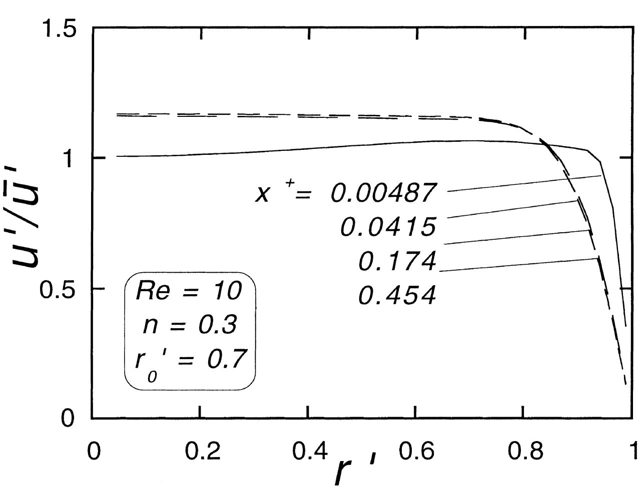


Fig. 2. Velocity profiles: Herschel–Bulkley material.

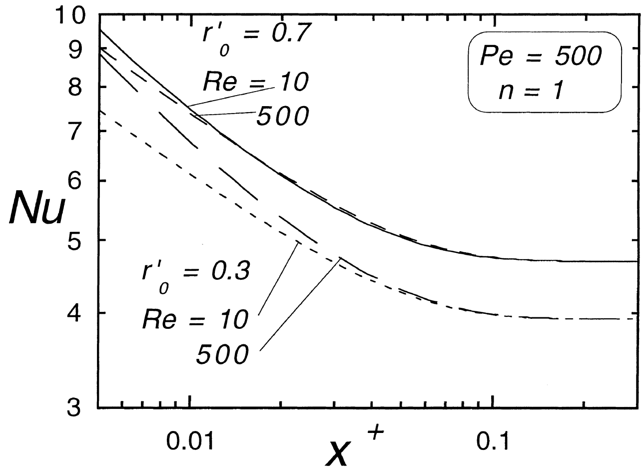


Fig. 6. Nu($x^+$) for different $r_0'$'s and Re's ($n = 1$, $T_w$ = const.).

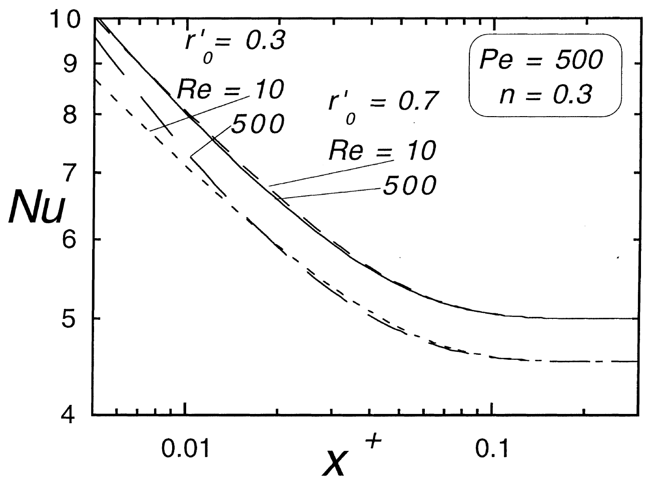


Fig. 7. Nu($x^+$) for different $r_0'$'s and Re's ($n = 0.3$, $T_w$ = const.).

Fig. 4 shows the Nusselt number variation with the inverse Graetz number, $x^+ \equiv x'/\mathrm{Pe}$, for a number of combinations of $r_0'$ and $n$. It is seen that high $r_0'$'s imply high velocity gradients near the wall, as does low $n$'s. For example, the curve for $r_0' = 0.7$ and $n = 0.3$ falls above all others in Fig. 4, while the curve for $r_0' = 0.3$ and $n = 1.0$ gives the lowest Nu for a given $x^+$. Thus, the combinations of $r_0'$ and $n$ which yield higher velocity gradients at the wall are the ones for which the Nusselt number is also higher, as expected.

Fig. 5 illustrates the entrance-region Nusselt number variation with the Peclet number, for some combinations of the governing parameters. It is interesting to observe that axial conduction is important in the vicinity of the tube inlet only, and its effect is to increase the Nusselt number. Larger yield stresses tend to decrease the axial conduction effect. On the other hand, axial conduction is not greatly affected by the power-law exponent in the range investigated.

For the constant-property situations examined in this paper, the Nusselt number depends on the material rheology through its influence on the velocity profile only. Therefore, axial diffusion of momentum – which affects the velocity field – is expected to affect the Nusselt number. This is illustrated in Figs. 6 and 7. It is seen in these figures that the effect is restricted to the neighborhood of the tube inlet, and is negligible for high yield stress materials. However, it becomes important as the rheological behavior approaches the Newtonian (higher $n$'s and lower $r_0'$'s).

Results are now shown for the uniform wall heat flux boundary condition. Fig. 8 shows temperature profiles at some axial locations, while Figs. 9–12 present Nusselt number results. Comparing these results with the ones obtained for the uniform wall temperature boundary condition, it is seen that the qualitative behavior is the same, both for the entrance region and for the fully developed portion of the flow. However, the Nusselt number values are much higher for the uniform wall heat flux boundary condition, as usual.

Finally, Figs. 13–16 illustrate the effect of property variation with temperature on the velocity profile and Nusselt number, for two different combinations of the flow parameters and for uniform wall heat flux. For both situations examined, the tube wall was assumed to be hotter than the flowing material. It can be observed that the velocity profile gets sharper near the wall for both cases, due to the fact that viscosity decreases in this region as a result of the wall heating. Therefore, the development length is larger when viscosity depends on the temperature. This effect on the velocity profile causes the Nusselt number to increase significantly in the entrance region. As the fully developed region is approached, the deviation gets smaller, since the radial temperature gradient (and hence the radial viscosity gradient) becomes milder.

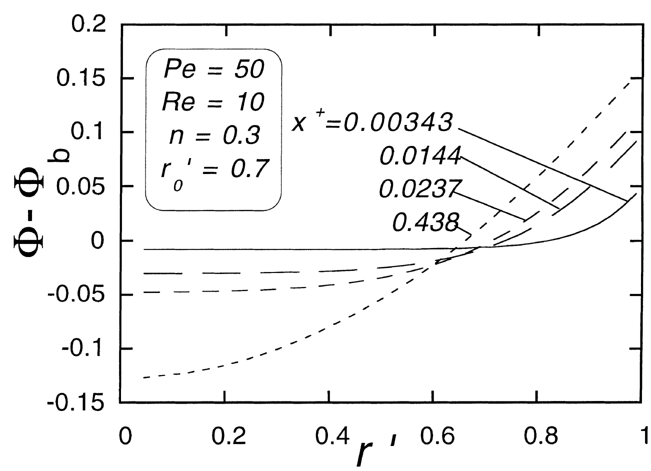


Fig. 8. Temperature profiles: Herschel–Bulkley material ($q_w$ = const.).

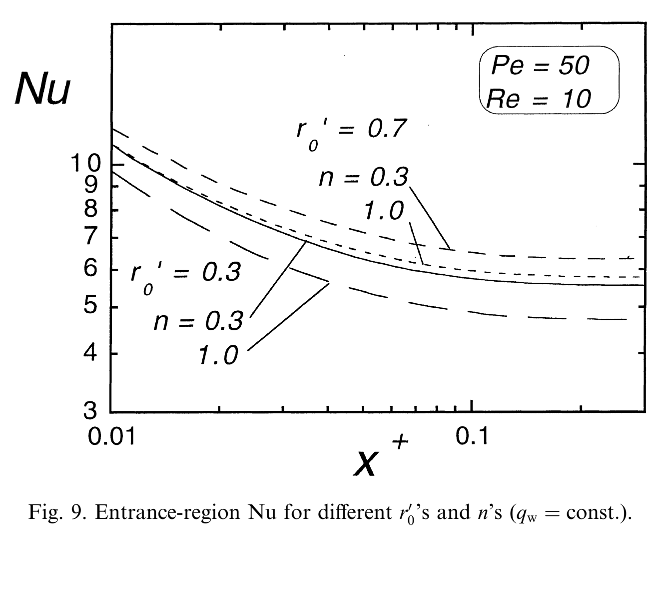


Fig. 9. Entrance-region Nu for different $r_0'$'s and $n$'s ($q_w$ = const.).

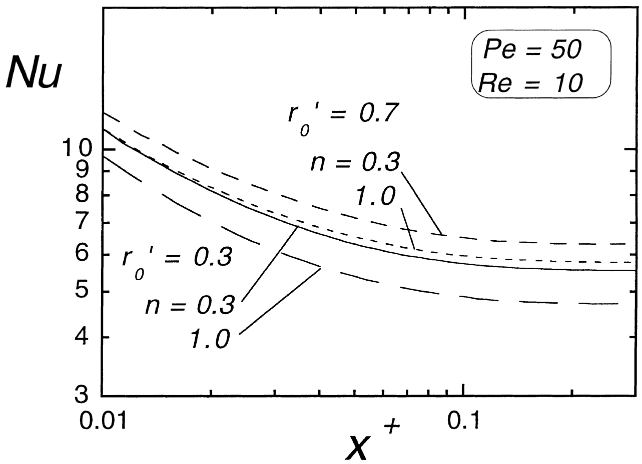


Fig. 10. Entrance-region Nu for different $r_0'$'s and Pe's ($q_w$ = const.).

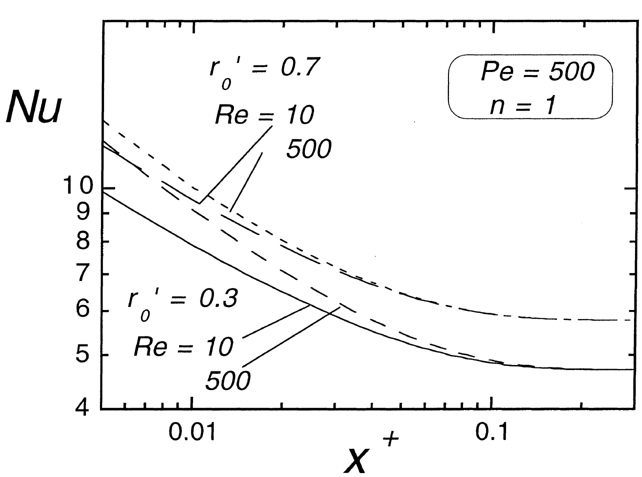


Fig. 11. Nu($x^+$) for different $r_0'$'s and Re's ($n = 1$, $q_w$ = const.).

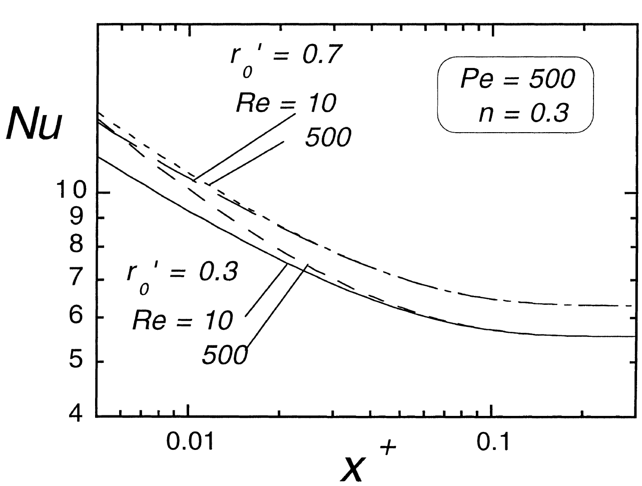


Fig. 12. Nu($x^+$) for different $r_0'$'s and Re's ($n = 0.3$, $q_w$ = const.).

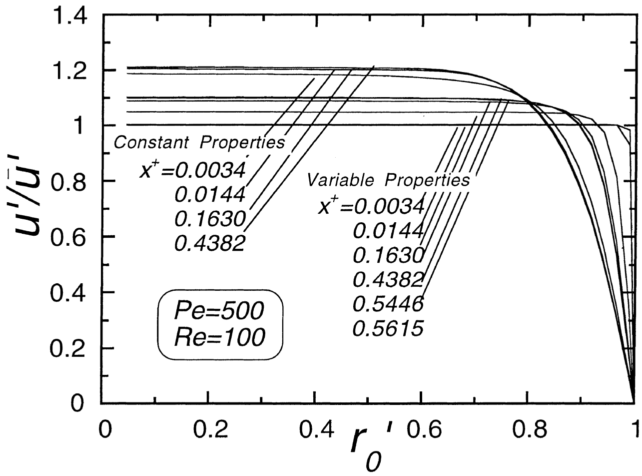


Fig. 13. Effect of variable properties on velocity (Re = 100, $q_w$ = const.).

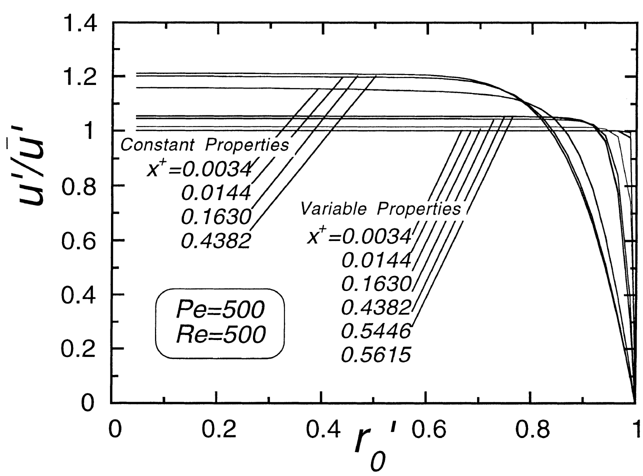


Fig. 14. Effect of variable properties on velocity (Re = 500, $q_w$ = const.).

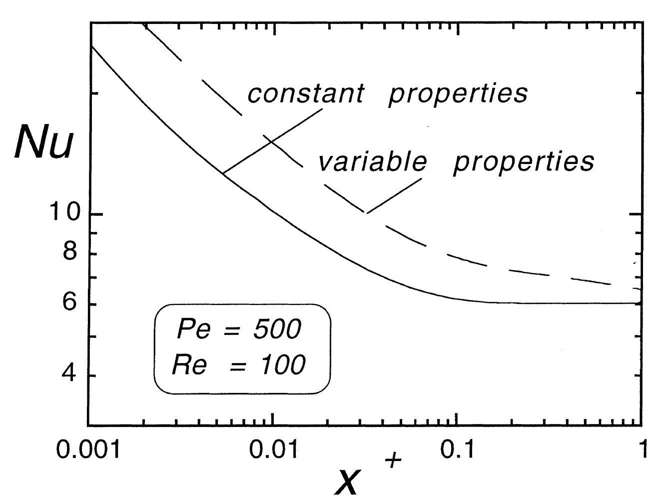


Fig. 15. Effect of variable properties on Nu (Re = 100, $q_w$ = const.).

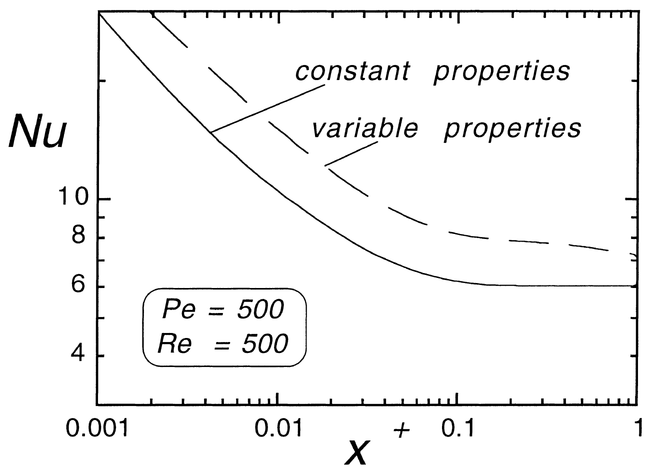


Fig. 16. Effect of variable properties on Nu (Re = 500, $q_w$ = const.).

## 4. Conclusions

Heat transfer in the entrance-region flow of the Herschel–Bulkley materials inside ducts is investigated. The case of simultaneous development of velocity and temperature profiles is analyzed. Both the uniform wall temperature and the uniform wall heat flux boundary conditions are examined.

The characteristic quantities employed are obtained from the fully developed analytical solution, which is presented in a new form. The form of the solution presented in this paper is more compact, and gives the velocity in terms of two convenient dimensionless parameters, namely, $n$ and $r_0'$.

The governing equations are solved numerically via a finite-volume technique. Results are presented in the form of velocity and temperature profiles, and entrance-region Nusselt number axial distributions.

In the entrance region the velocity profile presents an overshoot near the wall. The trends observed for temperature- and isoflux-wall boundary conditions are the same, but, as occurs in fully developed flows, the Nusselt number in the entrance region is always higher for the uniform wall heat flux case. It is also shown that the Nusselt number changes significantly in the entrance region due to the effect of property variation with temperature.

## Acknowledgements

Financial support for the present research was provided by Petrobras S.A., CNPq, FAPERJ and MCT.

## References

Abdali, S.S., Mitsoulis, E., Markatos, N.C., 1992. Entry and exit flows of Bingham fluids. J. Rheol. 36, 389.

Beverly, C.R., Tanner, R.I., 1992. Numerical analysis of three-dimensional Bingham plastic flow. J. Non-Newtonian Fluid Mechanics 42, 85–115.

Bird, R.B., Dai, G.C., Yarusso, B.J., 1983. The rheology of flows of viscoplastic materials. Rev. Chem. Eng. 1, 1–70.

Bird, R.B., Armstrong, R.C., Hassager, O. 1987. Dynamics of Polymeric Liquids, vol. 1, Wiley, New York.

Blackwell, B.F., 1985. Numerical solution of the Graetz problem for a Bingham plastic in laminar tube flow with constant wall temperature. Transactions ASME 107, 466–468.

Ellwood, K.R.J., Georgiou, G.C., Papanastasiou, C.J., Wilkes, J.O., 1990. Laminar jets of Bingham-plastic liquids. J. Rheol. 34, 787–812.

Forrest, G., Wilkinson, W.L., 1973. Laminar heat transfer to temperature-dependent Bingham fluids in tubes. Int. J. Heat Mass Transfer 16, 2377–2391.

Gartling, D.K., Phan-Thien, N., 1984. A numerical simulation of a plastic fluid in parallel-plate plastometer. J. Non-Newt. Fluid Mech. 14, 347–360.

Irvine Jr. T.F., Karni, J. 1987. Non-Newtonian fluid flow and heat transfer. In: Kakaç, S., Shah, R.K., Aung, W. (Eds.), Handbook of Single-Phase Convective Heat Transfer, Wiley, New York, 20.1–20.57.

Joshi, S.D., Bergles, A.E. 1980a. Experimental study of laminar heat transfer to in-tube flow of non-Newtonian fluids. J. Heat Transfer, 102, 397–401.

Joshi, S.D., Bergles, A.E. 1980b. Analytical study of laminar heat transfer to in-tube flow of non-Newtonian fluids. AICHE Symposium Series 199, 76, 270–81.

Lipscomb, G.G., Denn, M.M., 1984. Flow of Bingham fluids in complex geometries. J. Non-Newt. Fluid Mechanics 14, 337–346.

O'Donovan, E.J., Tanner, R.I., 1984. Numerical study of the Bingham squeeze film problem. J. Non-Newt. Fluid Mechanics 15, 75–83.

Nouar, C., Devienne, R., Lebouché, M., 1994. Convection thermique pour un fluide de Herschel-Bulkley dans la région d'entrée d'une conduite. Int. J. Heat Mass Transfer 37, 1–12.

Nouar, C., Lebouché, M., Devienne, R., Riou, C., 1995. Numerical analysis of the thermal convection for Herschel-Bulkley fluids. Int. J. Heat and Fluid Flow 16, 223–232.

Patankar, S.V. 1980. Numerical Heat Transfer and Fluid Flow, Hemisphere, Washington, DC.

Papanastasiou, T.C., 1987. Flows of materials with yield. J. Rheol. 31, 385–404.

Piau, J.M., 1996. Flow of a yield stress fluid in a long domain. Application to flow on an inclined plane. J. Rheol. 40, 711–723.

Richardson, S.M., 1987. Flows of variable-viscosity fluids in ducts with heated walls. J. Non-Newtonian Fluid Mechanics 25, 137–156.

Scirocco, V., Devienne, R., Lebouché, M., 1985. Écoulement laminaire et transfert de chaleur pour un fluide pseudo-plastique dans la zone d'entrée d'un tube. Int. J. Heat Mass Transfer 28, 91–99.

Settari, A., Aziz, K., 1973. A generalization of the additive correction methods for the iterative solution of matrix equations. SIAM J. Numerical Analyses 10, 506–521.

Shah, R.K., London, A.L., 1978. Laminar Flow Forced Convection in Ducts. Academic Press, New York.

Soares, M. 1996. Heat Transfer in Laminar Flow of Viscoplastic Materials through Short Tubes, M.S. Thesis, Department of Mechanical Engineering, Catholic University, Rio de Janeiro, Brazil (in Portuguese).

Soares, M., Souza, Mendes, P.R., Naccache, M.F. 1997. Heat Transfer to Viscoplastic Fluids in Laminar Flow Through Isothermal Short Tubes, Revista Brasileira de Ciências Mecânicas XIX, 1, pp. 1–14.

Souza Mendes, P.R., Naccache, M.F. 1995. Heat transfer to Herschel–Bulkley fluids in laminar fully developed flow through tubes. Proceedings of the COBEM-CIDIM 95, Belo Horizonte, Brazil (CD-ROM).

Vradis, G.C., Dougher, J., Kumar, S., 1992. Entrance pipe flow and heat transfer for a Bingham plastic. Int. J. Heat Mass Transfer 36, 543–552.

Van Doormaal, J.P., Raithby, G.D., 1984. Enhancements of the SIMPLE method for prediction incompressible fluid flows. Numerical Heat Transfer 7, 147–163.

Wilson, S.D.R., 1993. Squeezing flow of a yield-stress fluid in a wedge of slowly-varying angle. J. Non-Newt. Fluid Mechanics 50, 45–63.

Wilson, S.D.R., Taylor, A.J., 1996. The channel entry problem for a yield-stress fluid. J. Non-Newt. Fluid Mechanics 65, 165–176.